Supplement of Biogeosciences, 22, 1369–1391, 2025
https://doi.org/10.5194/bg-22-1369-2025-supplement

Biogeosciences Open Access EGU

Supplement of

Shifts in organic matter character and microbial assemblages from glacial headwaters to downstream reaches in the Canadian Rocky Mountains

Hayley F. Drapeau et al.

Correspondence to: Suzanne E. Tank (suzanne.tank@ualberta.ca)

Table S1: Site characteristics describing distance range, glacier source of headwaters, name of river, coordinates (in degrees, decimal minutes), approximate distance of sampling site from glacier terminus (estimated from Google Earth), and the number of times each site was visited in this study. Distance from glacier terminus and catchment coverage are as in Serbu et al. (2024).

Distance Range	Glacier headwaters	River	Latitude	Longitude	Distance from glacier terminus (km)	Number of times visited	Area	Catchment coverage (snow+ice / rock / forest)
Headwater	Athabasca	Sunwapta	52°12'25.8"	-117°14'05.9"	0.2	16	22.7	50.7 / 46.8 / 0.0
Near	Athabasca	Sunwapta	52°12'59.5"	-117°14'01.9"	1.7	15	29.3	41.8 / 54.2 / 0.3
Mid	Athabasca	Sunwapta	52°18'38.1"	-117°19'57.3"	15.5	17	198	19.1 / 55.3 / 12.8
Far	Athabasca	Sunwapta	52°31'58.7"	-117°38'39.2"	52.9	17	731	6.6 / 50.2 / 25.1
Far	Athabasca	Athabasca	52°34'59.6"	-117°44'21.9"	63.1	14	1635	12.2 / 43.2 / 27.3
Far	Athabasca	Athabasca	52°39'46.5”	-117°52'51.7"	73.9	18	1956	10.8 / 42.8 / 29.0
Far	Athabasca	Athabasca	52°48'43.4"	-118°02'33.2"	97.8	16	3020	8.4 / 41.2 / 32.0
Near	Saskatchewan	NSR	52°10'10.1"	-117°04'34.9"	5.6	18	76.2	54.7 / 35.5 / 3.6
Mid	Saskatchewan	NSR	52°4'9.1"	-116°54'54.9"	24.6	16	616	19.1 / 40.8 / 24.4
Mid	Saskatchewan	NSR	51°58'14.0"	-116°43'16.0"	46.3	16	1551	18.8 / 37.4 / 29.7
Near	Bow	Bow	51°39'42.3"	-116°29'13.0"	2.4	14	21.4	41.5 / 47.7 / 4.8
Mid	Bow	Bow	51°37'53.0"	-116°20'6.6"	17.1	15	105	11.1 / 42.0 / 31.4
Mid	Bow	Bow	51°25'43.2"	-116°11'20.4"	51.3	17	422	9.6 / 35.7 / 41.0
Far	Bow	Bow	51° 17' 5.82"	- 115° 59' 0.6"	75.4	13	1104	5.6 / 38.1 / 41.3

Table S2: Detection limits and methodological references for parameters assessed in this study. See also Serbu et al. (2024) for details.

Analyte	Detection limit	Method reference
TN	3 µg L^{-1}	EPA 353.2 (U.S. EPA, 1993b)
TP	1 µg L^{-1}	
NH_4^+	3 µg L^{-1}	SM 4500-NH3 (SM-APHAb)
TDN	3 µg L^{-1}	
TDP	1 µg L^{-1}	SM 4500-P (SM-APHAc)
SRP	1 µg L^{-1}	
NO_2^-+NO_3^-	2 µg L^{-1}	SM 4500-SiO2 (SM-APHAd)
Si	0.02 mg L^{-1}	
Mg^{2+}	0.05 mg L^{-1}	EPA 200.7 (U.S. EPA, 1994), SM 3125 (SM-APHAa)
Na^+	0.05 mg L^{-1}	
Ca^{2+}	0.05 mg L^{-1}	
K^+	0.05 mg L^{-1}	
Cl^-	0.03 mg L^{-1}	EPA 300.1 (U.S. EPA, 1993a)
SO_4^{2-}	0.04 mg L^{-1}	
Al^{3+}	0.49 µg L^{-1}	EPA 200.7, (U.S. EPA, 1994), SM 3125 (SM-APHAa)
Ba	0.05 µg L^{-1}	
Cr	0.02 µg L^{-1}	
Mn	0.04 µg L^{-1}	
Mo	0.01 µg L^{-1}	
Ni	0.02 µg L^{-1}	
Sr	0.04 µg L^{-1}	

Table S3: Description of characteristics for various the absorbance- and fluorescence-based metrics used in this study.

Measurement	Calculation	Purpose
$SUVA_{254}$	Normalization of UV absorbance at 254 nm to DOC	Increasing values indicate increasing aromaticity (Weishaar et al. 2003)
$S_{275\text{-}295}$	Slope over the 275nm-295nm wavelength range	Decreasing values indicates increasing molecular weight (Helms et al. 2008)
BIX	The ratio of emission at 380nm by 430nm at excitation of 310nm	Biological Index: Increasing values indicate recently produced organic carbon (Huguet et al. 2008)
HIX	Fluorescence intensity over 300-340nm divided by the combined fluorescence in the 300-345nm and 435-480nm	Humification Index; Increasing values indicate increasing humification (Ohno 2002)
FI	The ratio of emission at 400nm to 500nm at an excitation of 370nm	Fluorescence Index: Higher values indicate microbially derived fulvic acids, lower values indicate terrestrially derived fulvic acids (McKnight et al. 2001)

Table S4: Outputs of mixed effects models showing random effects and the fixed effect of distance based on the full model structure of *constituent ~ distance * melt.season + (1|river) + (1|year)*. Fixed effects of melt season and the interaction effect are not shown directly, but are reflected in the analysis of deviance. For the analysis of deviance outputs, probabilities <0.05 are highlighted in bold, and probabilities <0.10 are italicized. Where the effect of melt season was significant, post-hoc contrasts are shown in Table S5.

Constituent	**Random Effects**						**Fixed Effects**			**Analysis of Deviance**								
	River (Intercept)		Year (Intercept)		Residual		Distance			Distance			Melt Season			Interaction		
	Variance	SD	Variance	SD	Variance	SD	Estimate	SE	t-value	ChiSq	df	pr>ChiSq	ChiSq	df	pr>ChiSq	ChiSq	df	pr>ChiSq
d-excess	1.15E-01	3.39E-01	2.22E-03	4.71E-02	6.43E-01	8.02E-01	-1.91E-02	2.70E-03	-7.099	58.746	1	**0.000**	34.401	3	**0.000**	2.035	3	0.565
O-18	6.23E-02	2.50E-01	4.18E-02	2.05E-01	3.57E-01	5.98E-01	-1.16E-03	2.00E-03	-0.579	0.005	1	0.944	30.805	3	**0.000**	9.053	3	**0.029**
DOC	5.99E-03	7.74E-02	8.72E-03	9.34E-02	1.15E-01	3.39E-01	5.46E-03	1.05E-03	5.184	44.865	1	**0.000**	60.328	3	**0.000**	17.063	3	**0.001**
POC	1.13E-02	1.06E-01	3.89E-03	6.24E-02	1.60E-01	4.00E-01	5.34E-04	1.27E-03	0.420	0.569	1	0.451	5.195	3	0.158	1.194	3	0.754
%POC	9.71E-03	9.86E-02	2.77E-03	5.27E-02	2.47E-02	1.57E-01	-2.43E-03	5.59E-04	-4.353	18.308	1	**0.000**	23.152	3	**0.000**	3.242	3	0.356
Humic	2.43E-03	4.93E-02	3.08E-04	1.76E-02	3.77E-02	1.94E-01	3.68E-03	6.21E-04	5.929	43.959	1	**0.000**	22.602	3	**0.000**	0.734	3	0.865
13C-DOC	0	0	1.77E+00	1.33E+00	4.85E+00	2.20E+00	1.64E-02	6.88E-03	2.378	3.569	1	*0.059*	9.683	3	**0.022**	2.688	3	0.442
13C-POC	1.14E-09	3.37E-05	6.06E+00	2.46E+00	3.03E+00	1.74E+00	7.99E-03	4.83E-03	1.653	6.232	1	**0.013**	1.580	3	0.664	10.703	3	**0.013**
14C-DOC	2.84E-05	3.26E-04	6.56E+03	8.10E+01	1.44E+04	1.20E+02	3.81	2.12	1.795	6.033	1	**0.014**	23.704	3	**0.000**	1.285	3	0.733
14C-POC	0	0	1.01E+04	1.01E+02	1.08E+04	1.04E+02	-1.89	3.39	-0.557	0.461	1	0.497	3.283	2	0.194	2.656	3	0.265

Table S5: Post-hoc contrasts following significant effect of melt season in the models presented in Table S4.

				Estimate	SE	df	t-ratio	p-value
d-excess	Melt	-	PostMelt	0.53227	0.265	37.7	2.009	0.203
	Melt	-	PreMelt	1.09275	0.218	94.9	5.021	**<.001**
	Melt	-	Winter	0.00836	0.507	163.6	0.016	1.000
	PostMelt	-	PreMelt	0.56048	0.296	164	1.894	0.235
	PostMelt	-	Winter	-0.52391	0.528	182.4	-0.992	0.754
	PreMelt	-	Winter	-1.08439	0.525	184.3	-2.065	0.169
O-18	Melt	-	PostMelt	-0.56	0.194	174	-2.891	**0.022**
	Melt	-	PreMelt	0.613	0.153	187	3.995	**0.001**
	Melt	-	Winter	-0.371	0.375	187	-0.989	0.756
	PostMelt	-	PreMelt	1.173	0.217	187	5.393	**<.001**
	PostMelt	-	Winter	0.189	0.393	185	0.481	0.963
	PreMelt	-	Winter	-0.984	0.389	187	-2.531	*0.058*
DOC	Melt	-	PostMelt	0.2232	0.11	164	2.030	0.181
	Melt	-	PreMelt	-0.4948	0.081	188	-6.112	**<.001**
	Melt	-	Winter	0.1704	0.145	192	1.173	0.645
	PostMelt	-	PreMelt	-0.7179	0.121	190	-5.913	**<.001**
	PostMelt	-	Winter	-0.0528	0.174	192	-0.304	0.990
	PreMelt	-	Winter	0.6652	0.156	190	4.261	**<.001**
%POC	Melt	-	PostMelt	0.17317	0.0659	160	2.628	**0.046**
	Melt	-	PreMelt	0.17064	0.0413	166	4.134	**<.001**
	Melt	-	Winter	0.10376	0.1033	165	1.004	0.747
	PostMelt	-	PreMelt	-0.00253	0.0721	166	-0.035	1.000
	PostMelt	-	Winter	-0.06941	0.1216	166	-0.571	0.941
	PreMelt	-	Winter	-0.06689	0.1079	165	-0.620	0.926
Humic	Melt	-	PostMelt	0.1426	0.0641	86	2.223	0.125
	Melt	-	PreMelt	-0.1662	0.049	149	-3.394	**0.005**
	Melt	-	Winter	0.0864	0.1029	178	0.840	0.835
	PostMelt	-	PreMelt	-0.3088	0.075	135	-4.120	**<.001**
	PostMelt	-	Winter	-0.0561	0.1215	136	-0.462	0.967
	PreMelt	-	Winter	0.2527	0.1078	184	2.343	*0.092*
13C-DOC	Melt	-	PostMelt	-2.168	0.791	129	-2.740	**0.035**
	Melt	-	PreMelt	0.659	0.741	129	0.889	0.811
	Melt	-	Winter	4.236	9.642	129	0.439	0.972
	PostMelt	-	PreMelt	2.826	1.087	129	2.600	*0.050*
	PostMelt	-	Winter	6.404	9.673	130	0.662	0.911
	PreMelt	-	Winter	3.577	9.66	129	0.370	0.983
14C-DOC	Melt	-	PostMelt	3.72	99.8	39.9	0.037	1.000
	Melt	-	PreMelt	-9.69	68	38.9	-0.142	0.999
	Melt	-	Winter	408.70	96	38.5	4.257	**0.001**
	PostMelt	-	PreMelt	-13.4	121.3	40.5	-0.111	1.000
	PostMelt	-	Winter	404.99	139.1	40.1	2.912	**0.029**
	PreMelt	-	Winter	418.39	105.7	37.2	3.959	**0.002**

Table S6: Excitation and emission maxima associated with PARAFAC components and associated DOM character as assessed by cross reference with the Open Fluor database.

Component	Emission peak	Excitation peak	Character	Number of Open Fluor Matches
C1	271	230	Terrestrial / humic (Shutova et al., 2014)	118
C2	409	230	Terrestrial / humic (Catalán et al., 2018; Coulson et al., 2022; Shutova et al., 2014)	105
C3	340	230	Microbial/tryptophan like (Murphy et al., 2008; Stedmon & Markager, 2005)	27
C4	300	230, 270-275	Microbial/tyrosine like(Graeber et al., 2012)	14

Table S7: perMANOVA test outputs showing the variation between proportion of microbial communities by distance range, hydrological season, year, and river. perMANOVA pairwise comparisons with holm adjusted p values are shown. Significant interactions are bolded.

Factor	**R^2**	**significance**	**PERMANOVA pairwise comparison**	**p (Holms adjusted)**
Distance Range	0.09	< 0.001	Headwater - Near	0.1659
			Headwater - Far	**0.0044**
			Near - Far	**0.0003**
Year	0.08	<0.001	2019-2020	**0.0003**
			2019-2021	**0.0024**
			2020-2021	**0.0068**
Season	0.06	0.002	PreMelt – Melt	**0.0039**
			PreMelt – PostMelt	0.0602
			Melt – PostMelt	0.2125
River	0.08	<0.001	Sunwapta-Athabasca	**0.0027**
			Sunwapta-NSR	**0.0003**
			Athabasca-NSR	**0.0003**

Table S8: Potential OC sources to glacially-influenced streams, and their associated expected fluorescence signature and δ^{13}C-OC and Δ^{14}C-OC ranges.

Source	**δ^{13}C-OC**	**Δ^{14}C-OC**	**Expected DOM fluorescence**
Vegetation	-26 to -28‰ (Peterson and Fry, 1987)	Downstream (contemporary) vegetation will be modern whereas subglacial over-ridden vegetation likely represents an aged OC source (Bhatia et al., 2013)	Humic-like (Gabor et al., 2014)
Soils and associated pore water	-26 to -28‰ (Peterson and Fry, 1987)	Modern at the surface with increasing age with depth (Shi et al., 2020)	Humic-like with decreasing humification and increasing protein-like fluorescence with depth and increased soil residence time (Gabor et al., 2014) (McDonough et al., 2022)
Phytoplankton	-22 to -30‰ (Chanton & Lewis, 1999)	Ranging from modern to slightly aged depending on CO_2 source	Protein-like (Fellman et al., 2010)
Benthic algae	Greater than -7 to -15‰ due to decreased isotopic fractionation, following carbon limitation associated with benthic boundary layers (Hecky & Hesslein, 1995)	Ranging from modern to slightly aged depending on CO_2 source	Protein-like (Fellman et al., 2010)
Fossil fuel deposits	-27‰ (Peterson & Fry, 1987)	Ancient (radiocarbon dead)	Variable (Mladenov et al., 2010)
Wildfire derived soot	-26 to -28‰ (Peterson & Fry, 1987)	Modern (Masiello & Druffel, 2003)	Variable (Mladenov et al., 2010)
Chemosynthesis	Very depleted -30 to -80‰, via sulfur oxidizing and methanogenic microbes (Blaser & Conrad, 2016; Rau & Hedges, 1979; Ruby et al., 1987)	Ranging from modern to slightly aged depending on the CO_2 source. Notably, subglacial CO_2 can represent an aged C source	Protein-like (Fellman et al., 2010)

Table S9: Overview of all sample codes used in this study, with corresponding river (Sunwapta, Athabasca, North Saskatchewan, Bow), distance downstream, and month and year of sampling. "E" and "L" refers to samples collected early, and late, in June 2020.

Sample ID	River_Distance_MMYY	Sample ID	River_Distance_MMYY
R19_04	S_52.9_0519	R20_61	S_52.9_0920
R19_05	A_73.9_0519	R20_71	A_97.8_1020
R19_06	A_97.8_0519	R20_73	S_1.7_1020
R19_09	N_5.6_0519	R20_75	S_52.9_1020
R19_25	A_63.1_0719	R21_01	S_52.9_0121
R19_29	S_1.7_0719	R21_03	A_73.9_0121
R19_31	S_52.9_0719	R21_05	A_63.1_0521
R19_39	A_63.1_0819	R21_06	A_73.9_0521
R19_41	A_97.8_0819	R21_07	A_97.8_0521
R19_43	S_1.7_0819	R21_08	S_0.2_0521
R19_45	S_52.9_0819	R21_09	S_1.7_0521
R19_46	N_5.6_0819	R21_11	S_52.9_0521
R19_57	S_1.7_1019	R21_12	N_5.6_0521
R19_59	S_52.9_1019	R21_18	A_63.1_0621
R20_02	S_1.7_0620E	R21_19	A_73.9_0621
R20_04	S_52.9_0620E	R21_20	A_97.8_0621
R20_05	A_63.1_0620E	R21_21	S_0.2_0621
R20_06	A_73.9_0620E	R21_22	S_1.7_0621
R20_07	A_97.8_0620E	R21_24	S_52.9_0621
R20_08	N_5.6_0620E	R21_25	N_5.6_0621
R20_15	A_73.9_0620L	R21_34	A_97.8_0721
R20_16	A_97.8_0620L	R21_38	S_52.9_0721
R20_19	S_52.9_0620L	R21_39	N_5.6_0721
R20_20	N_5.6_0620L	R21_45	A_63.1_0821
R20_28	A_73.9_0720	R21_46	A_73.9_0821
R20_29	A_97.8_0720	R21_47	A_97.8_0821
R20_30	S_0.2_0720	R21_48	S_0.2_0821
R20_31	S_1.7_0720	R21_49	S_1.7_0821
R20_33	S_52.9_0720	R21_51	S_52.9_0821
R20_34	N_5.6_0720	R21_52	N_5.6_0821
R20_42	A_73.9_0820	R21_61	A_97.8_0921
R20_47	S_52.9_0820	R21_62	S_0.2_0921
R20_48	N_5.6_0820	R21_63	S_1.7_0921
R20_55	A_63.1_0920	R21_65	S_52.9_0921
R20_56	A_73.9_0920	R21_66	N_5.6_0921
R20_58	S_0.2_0920	R21_snow	Sn

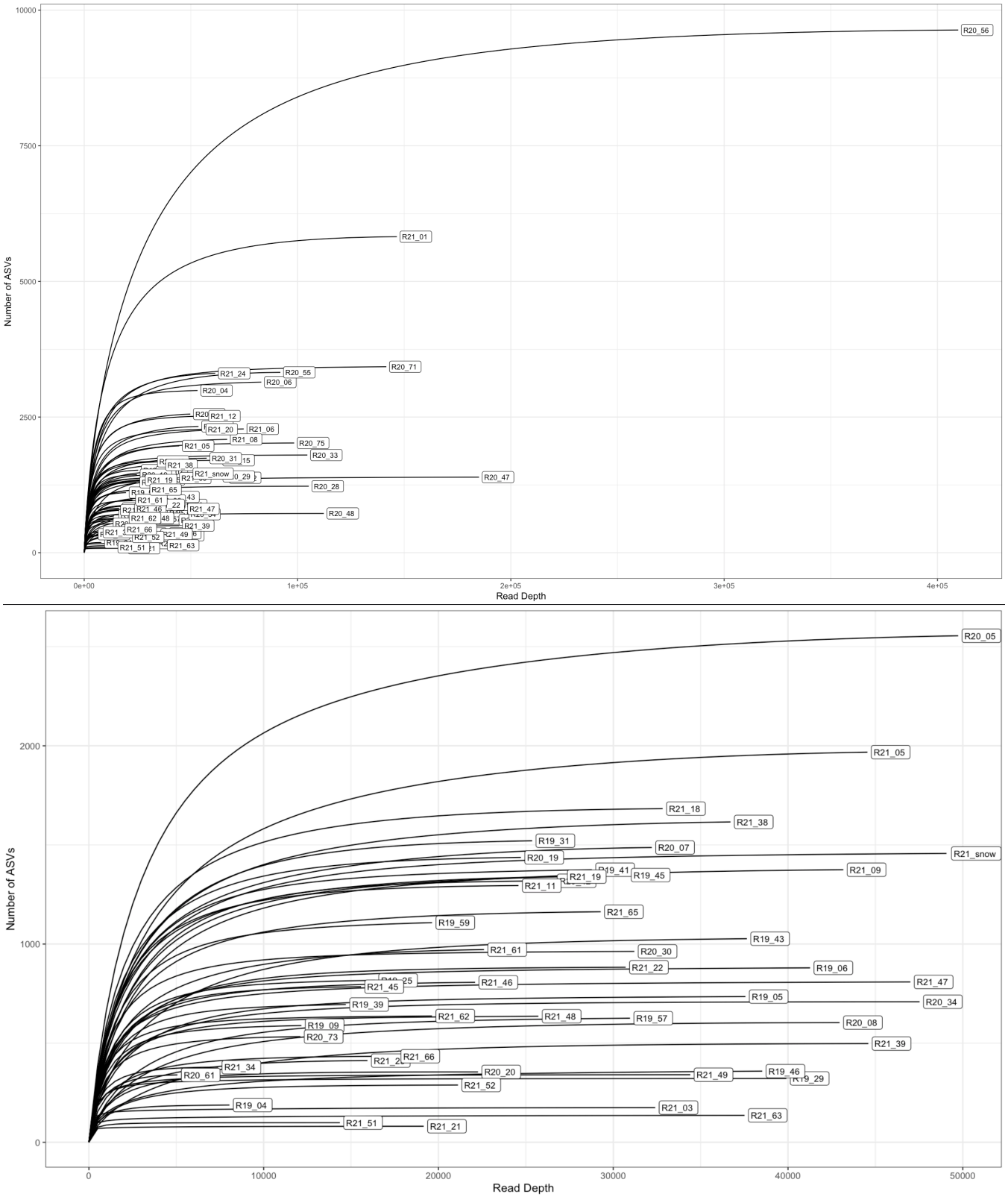

Figure S1: Rarefaction curves to show read depth relative to ASV count for individual samples collected during this study. The top panel shows all samples. The bottom panel shows only samples with a read depth of less than 50,000. Samples with read depths of less than 5,000 were excluded, and are therefore not shown in these plots. Sample codes correspond with rivers and dates in Table S9.

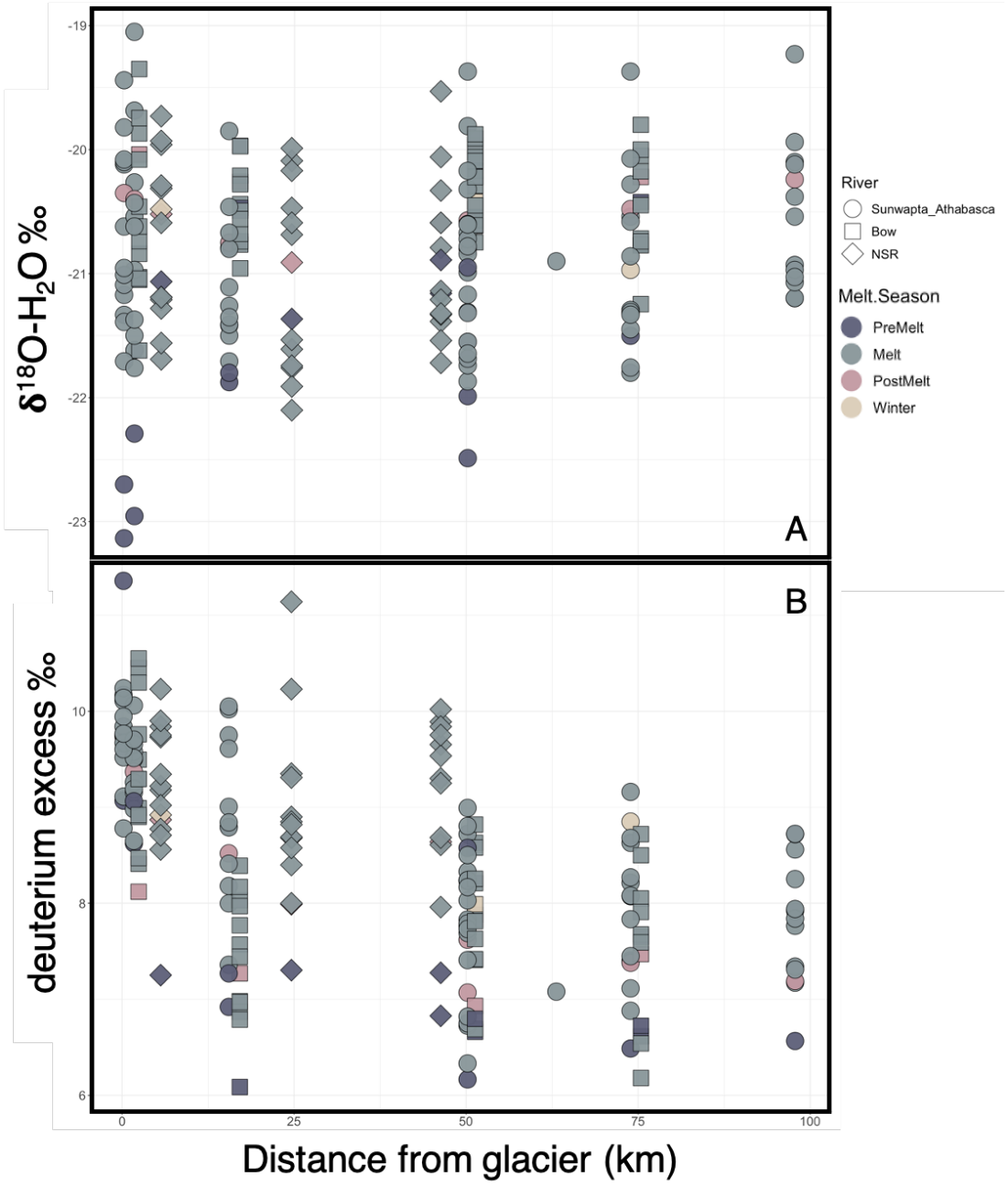

Figure S2: Plots of (A) $\delta^{18}O$-H_2O, and (B) deuterium excess with increasing distance downstream from glacial terminus. Melt season and river are indicated.

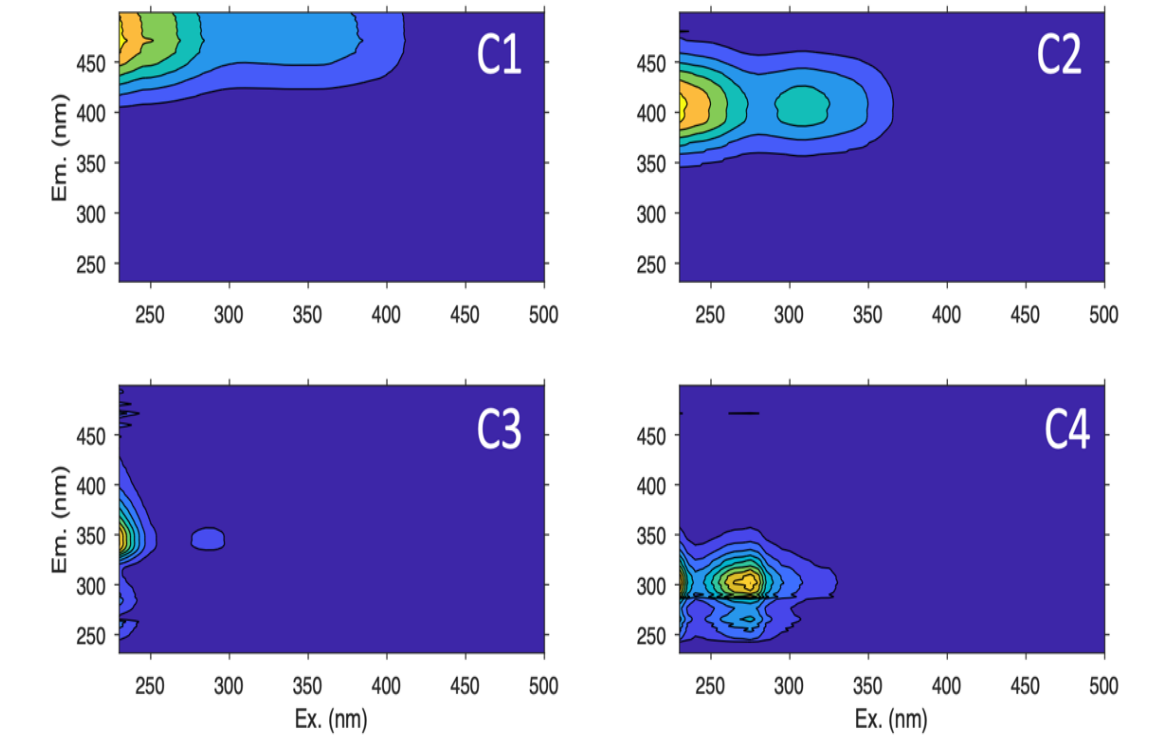

Figure S3: Component plots for the four-component PARAFAC model

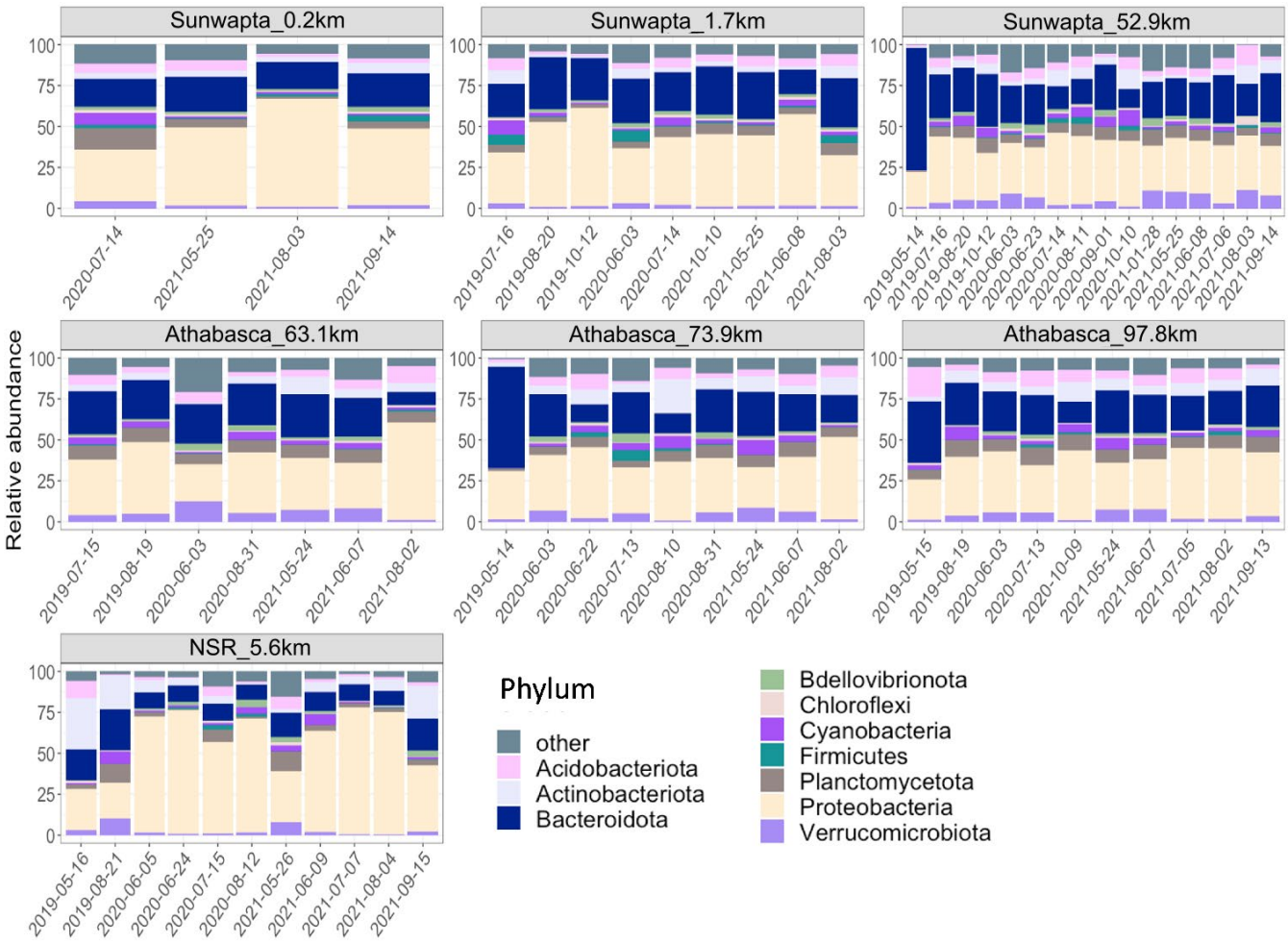

Figure S4: Relative abundance of the top ten most abundant phyla across all sampling dates at headwater, near and far sites in the Sunwapta-Athabasca and North Saskatchewan rivers. The category "Other" represents classes not included in the top ten.

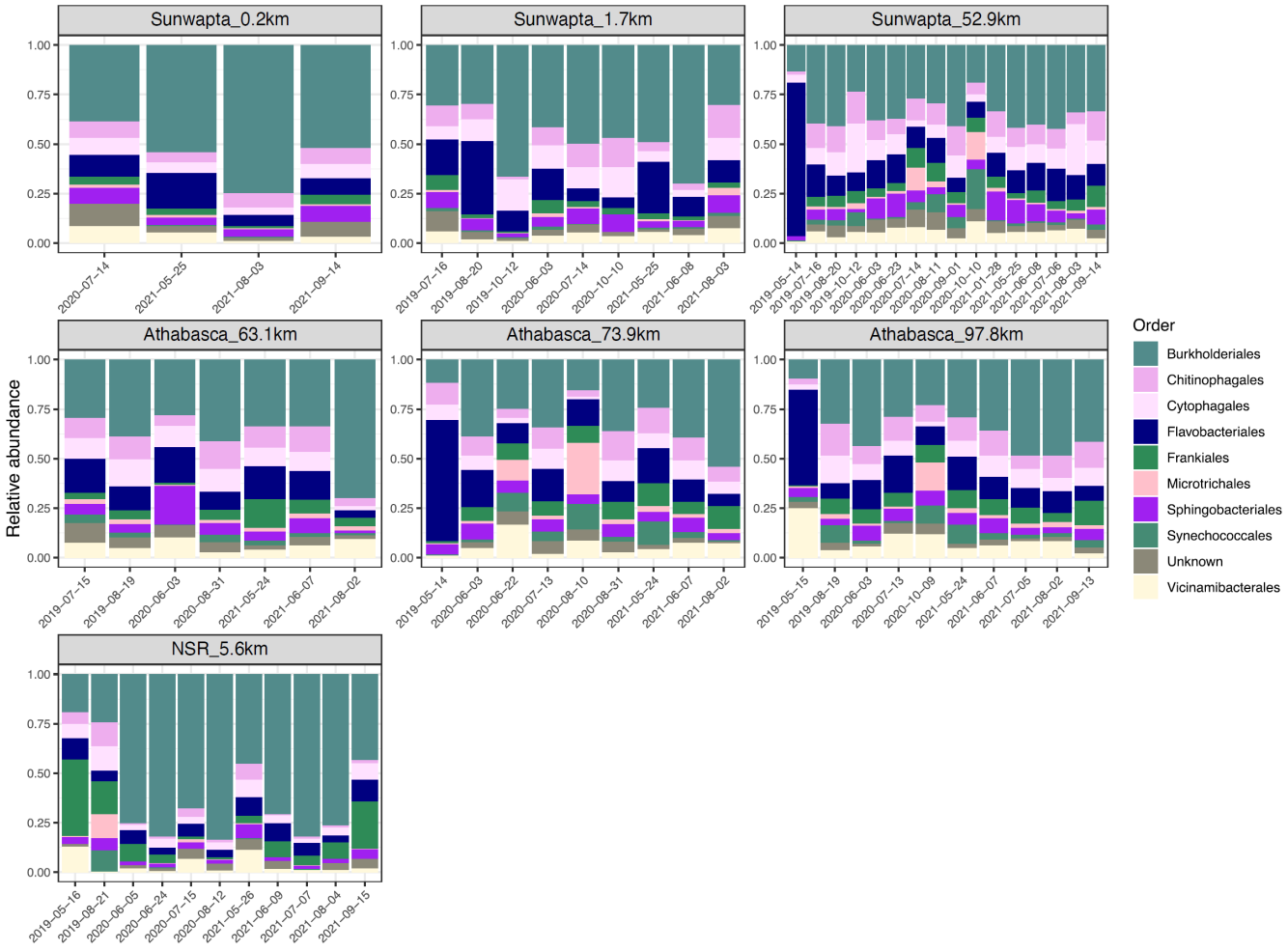

Figure S5: Relative abundance of the top ten most abundant orders across all sampling dates at the near and far sites in the Sunwapta-Athabasca and North Saskatchewan rivers. The category "Other" represents classes not included in the top ten.

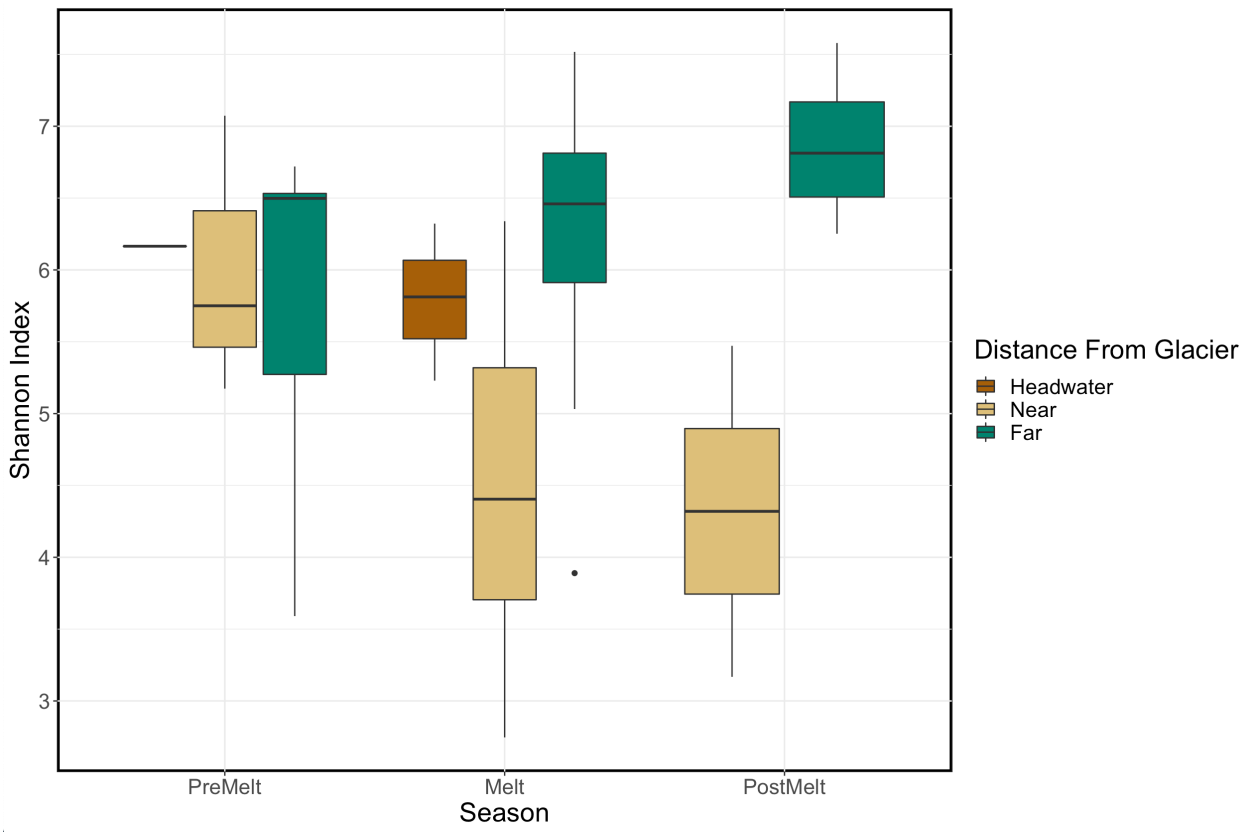

Figure S6: Boxplots showing variation in alpha diversity across hydrological periods and distance range, using the Shannon diversity index. The boxes represent the interquartile range, the black line represents the median value, and the points represent outliers.

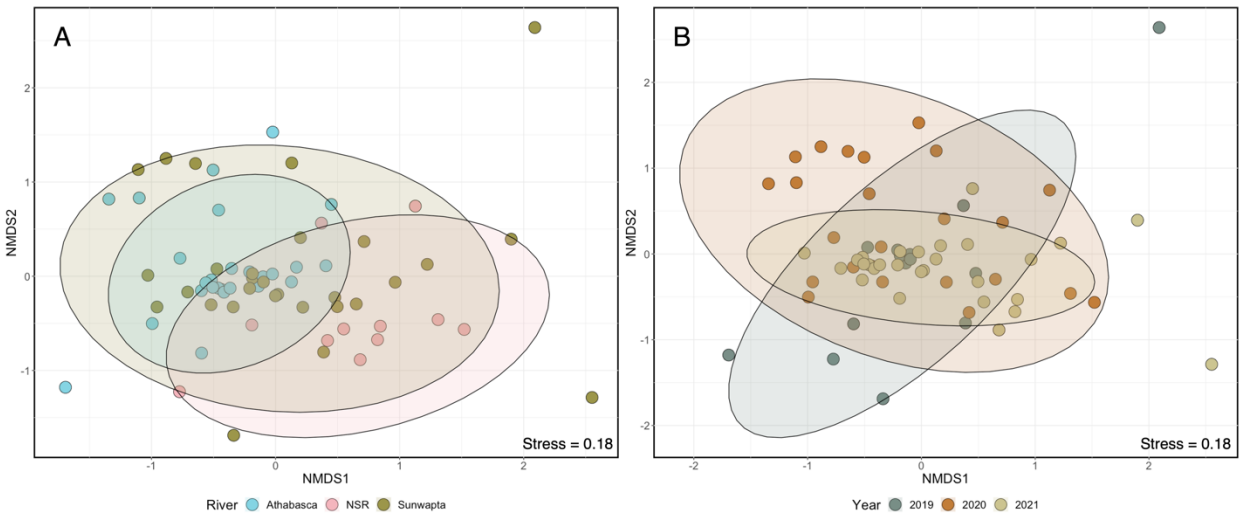

Figure S7: NMDS of microbial assemblage composition based on Bray Curtis distances of Hellinger transformed ASV data. Colour represents different (A) study rivers and (B) sampling years. Shaded circles represent the 95% confidence interval for significantly different groupings (pairwise perMANOVA $p < 0.01$ (Holm's adjusted) see Table S7).

References:

Bhatia, M. P., Das, S. B., Xu, L., Charette, M. A., Wadham, J. L., & Kujawinski, E. B. (2013). Organic carbon export from the Greenland ice sheet. *Geochimica et Cosmochimica Acta*, *109*, 329–344. https://doi.org/10.1016/j.gca.2013.02.006

Blaser, M., & Conrad, R. (2016). Stable carbon isotope fractionation as tracer of carbon cycling in anoxic soil ecosystems. *Current Opinion in Biotechnology*, *41*, 122–129. https://doi.org/10.1016/j.copbio.2016.07.001

Chanton, J. P., & Lewis, F. G. (1999). Plankton and dissolved inorganic carbon isotopic composition in a river-dominated estuary: Apalachicola Bay, Florida. *Estuaries*, *22*(3), 575–583. https://doi.org/10.2307/1353045

Gabor, R. S., Baker, A., McKnight, D. M., & Miller, M. P. (2014). Fluorescence Indices and Their Interpretation. In A. Baker, D. M. Reynolds, J. Lead, P. G. Coble, & R. G. M. Spencer (Eds.), *Aquatic Organic Matter Fluorescence* (pp. 303–338). Cambridge University Press. https://doi.org/10.1017/CBO9781139045452.015

Fellman, J. B., Hood, E., & Spencer, R. G. M. (2010). Fluorescence spectroscopy opens new windows into dissolved organic matter dynamics in freshwater ecosystems: A review. *Limnology and Oceanography*, *55*(6), 2452–2462. https://doi.org/10.4319/lo.2010.55.6.2452

Hecky, R. E., & Hesslein, R. H. (1995). Contributions of Benthic Algae to Lake Food Webs as Revealed by Stable Isotope Analysis. *Journal of the North American Benthological Society*, *14*(4), 631–653. https://doi.org/10.2307/1467546

Masiello, C. A., & Druffel, E. R. M. (2003). Organic and black carbon 13C and 14C through the Santa Monica Basin sediment oxic-anoxic transition. *Geophysical Research Letters*, *30*(4). https://doi.org/10.1029/2002GL015050

McDonough, L. K., Andersen, M. S., Behnke, M. I., Rutlidge, H., Oudone, P., Meredith, K., O'Carroll, D. M., Santos, I. R., Marjo, C. E., Spencer, R. G. M., McKenna, A. M., & Baker, A. (2022). A new conceptual framework for the transformation of groundwater dissolved organic matter. *Nature Communications*, *13*(1), Article 1. https://doi.org/10.1038/s41467-022-29711-9

Mladenov, N., Reche, I., Olmo, F. J., Lyamani, H., & Alados-Arboledas, L. (2010). Relationships between spectroscopic properties of high-altitude organic aerosols and Sun photometry from ground-based remote sensing. *Journal of Geophysical Research: Biogeosciences*, *115*(G1). https://doi.org/10.1029/2009JG000991

Peterson, B. J., & Fry, B. (1987). Stable Isotopes in Ecosystem Studies. *Annual Review of Ecology and Systematics*, *18*(1), 293–320. https://doi.org/10.1146/annurev.es.18.110187.001453

Rau, G. H., & Hedges, J. I. (1979). Carbon-13 depletion in a hydrothermal vent mussel: Suggestion of a chemosynthetic food source. *Science (New York, N.Y.)*, *203*(4381), 648–649. https://doi.org/10.1126/science.203.4381.648

Ruby, E. G., Jannasch, H. W., & Deuser, W. G. (1987). Fractionation of Stable Carbon Isotopes during Chemoautotrophic Growth of Sulfur-Oxidizing Bacteria. *Applied and Environmental Microbiology*, *53*(8), 1940–1943.

Serbu, J. A., St. Louis, V. L., Emmerton, C. A., Tank, S. E., Criscitiello, A. S., Silins, U., et al. (2024). A comprehensive biogeochemical assessment of climate-threatened glacial river headwaters on the eastern slopes of the Canadian Rocky Mountains. Journal of Geophysical Research: Biogeosciences, 129, e2023JG007745. https://doi.org/10.1029/2023JG007745

Standard Methods Committee of the American Public Health Association, American Water Works Association, & Water Environment Federation. (2018a). Method 3125: Metals by Inductively

Coupled Plasma-Mass Spectrometry (ICP-MS). In W. C. Lipps, T. E. Baxter, & E. Braun-Howland (Eds.), Standard Methods for the Examination of Water and Wastewater. APHA Press. https://doi.org/10.2105/smww.2882.048

Shi, Z., Allison, S. D., He, Y., Levine, P. A., Hoyt, A. M., Beem-Miller, J., Zhu, Q., Wieder, W. R., Trumbore, S., & Randerson, J. T. (2020). The age distribution of global soil carbon inferred from radiocarbon measurements. *Nature Geoscience*, *13*(8), Article 8. https://doi.org/10.1038/s41561-020-0596-z

Standard Methods Committee of the American Public Health Association, American Water Works Association, & Water Environment Federation. (2018b). Method 4500-NH3 (Ammonia). In W. C. Lipps, T. E. Baxter, & E. Braun-Howland (Eds.), Standard Methods for the Examination of Water and Wastewater. APHA Press. https://doi.org/10.2105/SMWW.2882.087

Standard Methods Committee of the American Public Health Association, American Water Works Association, & Water Environment Federation. (2018c). Method 4500-P (Phosphorus). In W. C. Lipps, T. E. Baxter, & E. Braun-Howland (Eds.), Standard Methods for the Examination of Water and Wastewater. APHA Press.

Standard Methods Committee of the American Public Health Association, American Water Works Association, & Water Environment Federation. (2018d). Method 4500-SiO2 (Silica). In W. C. Lipps, T. E. Baxter, & E. Braun-Howland (Eds.), Standard Methods for the Examination of Water and Wastewater. APHA Press. https://doi.org/10.2105/SMWW.2882.095

U.S. EPA. (1993a). Method 300.1: Determination of anions in drinking water by ion chromatography. In Methods for the Determination of Organic and Inorganic Compounds in Drinking Water (EPA 815/R-00-014). U.S. EPA Federal Registry.

U.S. EPA. (1993b). Method 353.2: Determination of nitrate-nitrite nitrogen by automated colorimetry. In Methods for Chemical Analysis of Water and Wastes (EPA 600/4-79-020). U.S. EPA Federal Registry.

U.S. EPA. (1994). Method 200.7, Revision 4.4: Determination of metals and trace elements in water and wastes by Inductively Coupled Plasma-Atomic Emission Spectrometry (ICP-AES). U.S. EPA Federal Registry.